Israel Journal of Plant Sciences *Vol. 60* *2012* *pp. 107–121*
DOI: 10.1560/IJPS.60.1-2.107

Estimating radiation interception in an olive orchard using physical models and multispectral airborne imagery

M.L. Guillén-Climent,[a] P.J. Zarco-Tejada,[a,*] and F.J. Villalobos[a,b]
[a]*Instituto de Agricultura Sostenible (IAS), Consejo Superior de Investigaciones Científicas (CSIC), Alameda del Obispo, s/n, 14004-Córdoba, Spain*
[b]*Departamento de Agronomía, Universidad de Córdoba (UCO), Córdoba, Spain*

(*Received 12 August 2011*; *accepted in revised form 6 November 2011*)

Honoring Anatoly Gitelson on the occasion of his 70th birthday

ABSTRACT

This study was conducted to estimate the fraction of Intercepted Photosinthetically Active Radiation (fIPAR) in an olive orchard. The method proposed to estimate fIPAR in olive canopies consisted of a coupled radiative transfer model that linked the 3D *Forest Light Interaction Model* (FLIGHT) and the *Orchard Radiation Interception Model* (ORIM). This method was used to assess the estimation of instantaneous fIPAR as a function of planting grids, percentage cover, and soil effects. The linked model was tested against field measurements of fIPAR acquired for a commercial olive orchard, where study plots showing a gradient in the canopy structure and percentage cover were selected. High-resolution airborne multispectral imagery was acquired at 10 nm bandwidth and 15-cm spatial resolution, and the reflectance used to calculate vegetation indices from each study site. In addition, simulations of the land surface bidirectional reflectance were conducted to understand the relationships between canopy architecture and fIPAR on typical olive orchard planting patterns. Input parameters used for the canopy model, such as the leaf and soil optical properties, the architecture of the canopy, and sun geometry, were studied in order to assess the effect of these inputs on the *Normalized Difference Vegetation Index* (NDVI) and fIPAR relationships. FLIGHT and ORIM models were independently assessed for fIPAR estimation using structural and ceptometer field data collected from each study site, yielding RMSE values of 0.1 for the FLIGHT model, while the specific olive simulation model by ORIM yielded lower errors (RMSE = 0.05). The reflectance simulations conducted as a function of the orchard architecture confirmed the usefulness of the modeling methods for this heterogeneous olive crop, and the high sensitivity of the NDVI and fIPAR to background, percentage cover, and sun geometry on these heterogeneous orchard canopies. The fIPAR estimations obtained from the airborne imagery through predictive relationships yielded RMSE error values of 0.11 when using FLIGHT to simulate both the canopy reflectance and the fIPAR of the study sites. The coupled FLIGHT+ORIM model yielded better results, obtaining RMSE = 0.05 when using airborne remote sensing imagery to estimate fIPAR.

Keywords: olive orchards, remote sensing, fIPAR estimation, radiative transfer modeling

*Author to whom correspondence should be addressed.
E-mail: pzarco@ias.csic.es

1. INTRODUCTION

The olive industry have experimented with several major technological changes during the last two decades (Villalobos et al., 2006). Traditional olive groves, grown in rain-fed conditions with low density (80–90 olive trees/ha), have been very well adapted and able to survive periods of intense drought with acceptable production (Pastor et al., 2007; Fernandes-Silva et al., 2010). Nevertheless, such traditional olive orchards are being substituted by new intensive, drip irrigated and fertilized planting for high early yields (Beede and Goldhammer, 1994; Villalobos et al., 2006; Pastor et al., 2007). This transition requires a better understanding of the olive orchard, including longer term effects of these structural changes to better adapt the required management for these canopies. Therefore, the interest by the research community in olive tree cultivation and management practices is growing, considering the historical importance of this crop throughout the Mediterranean countries (Vossen, 2007; Ben-Gal et al., 2011). A comprehensive review of scientific research in olive crops can be found in Connor and Fereres (2005). In this study, the authors emphasized that future research should prioritize studies of olive trees as a whole, rather than just leaf-level analyses. Subsequent studies conducted in olive orchards have focused on optimizing water use at tree level (Testi et al., 2006; Orgaz et al., 2007; Iniesta et al., 2009; Fernandes-Silva et al., 2010), optimizing the tree density (Pastor et al., 2007), or determining biophysical parameters (Gómez et al., 2011). Some of these studies used the *Orchard Radiation Interception Model* (ORIM) to estimate the fraction of Intercepted Photosinthetically Active Radiation (fIPAR) in olive orchards (Mariscal et al., 2000). The rationale is that a first step in productivity assessment is the estimation of radiation interception (Connor and Fereres, 2005), therefore requiring simulation models to quantify the relationships with the orchard architecture. In fact, biomass production is directly related to the intercepted radiation (Monteith, 1977), and this has been shown to be true for olive canopies (Mariscal et al., 2000). Therefore, the use of crop simulation models is required as a consequence of the wide variability and complexity of these canopies (Villalobos et al., 2006). The field measurements of IPAR and/or the related fraction of intercepted PAR (fIPAR) would be inefficient and time consuming in these orchards. The large variation that olive orchards show in tree dimensions, canopy architecture, and ground cover are a consequence of the transformation from rain-fed to irrigation schemes, with high density in areas of chronic water shortages (Testi et al., 2006). Moreover, olive tree orchards are grown as horizontally non-homogeneous canopies, and the amount of PAR intercepted is defined by the combination of tree spacing (row and inter-row), tree height, row orientation, vertical projection of the canopy cover, and canopy volume (Connor and Fereres, 2005). In this context, along with radiative transfer modelling efforts, remote sensing methods are useful for the assessment of large areas and to map the within-field and between-orchard spatial variability of biophysical parameters.

This study is focused on the estimation of the IPAR in olive orchards using remote sensing imagery and radiative transfer modelling methods. In other studies, empirical and modelled relationships between vegetation indices and fIPAR have been developed for homogeneous canopies, such as wheat, maize, or soybean crops (e.g., Daughtry et al., 1983; Asrar et al., 1984; Wiegand et al., 1991; Hall et al., 1992; Moriondo et al., 2007) and forest canopies (e.g., Myneni and Williams, 1994; Roujean and Breon, 1995; Huemmrich and Goward, 1997; De Castro and Fetcher, 1998; Huemmrich, 2001; and Zhang et al., 2009). With the development of 3D canopy reflectance models, the sensitivity of the relationships between vegetation indices and the fraction of PAR, absorbed or intercepted, can be investigated using architectural characteristics of the canopy. However, these studies—focused on herbaceous crops and closed-canopy forestry areas—are not applicable to non-homogeneous, open-canopy olive orchards. In general, the monitoring of fIPAR and fAPAR during the course of the day and the growing season is of central interest to determine net photosynthesis and dry matter production (Olofsson and Eklundh, 2007). However, a first step to model the implications of the structure on the instantaneous fIPAR requires appropriate simulation methods to account for the canopy optical properties and background. In fact, previous works indicated that the use of radiative transfer models capable of handling row orientations is a requisite for remote sensing in horticulture (Kempeneers et al., 2008; Stuckens et al., 2009). Among these efforts, radiative transfer models that aim at deriving the amount and distribution of fIPAR in non-homogeneous crop canopies have been reviewed by Mariscal et al. (2000), who developed a model to simulate fIPAR in olive orchard canopies. Later, other models were developed on different types of orchard configuration such as hedgerow, overhead training, or isolated trees (Friday and Fowness, 2001; Annadale et al., 2004; Oyarzun et al., 2007). However, none of them make use of remote sensing imagery to estimate radiation interception remotely. The 3D Forest Light Interaction Model (FLIGHT) (North, 1996) was proposed to estimate fAPAR in forest canopies (North, 2002; Prieto-Blanco et al., 2009), and more recently

in orange and peach canopies (Guillén-Climent et al., 2012). While methods for modeling and estimating fIPAR in homogenous vegetation are relatively mature (Mariscal et al., 2000), further research is needed for robust estimate of fIPAR in open canopies. The objectives of this study were: (i) to evaluate modelling strategies for estimating instantaneous fIPAR in olive orchards; and (ii) to use remote sensing imagery and modeling methods to estimate instantaneous fIPAR in olive canopies using visible (VIS) and near-infrared (NIR) bands, as well as to generate a map of the spatial variability of fIPAR.

2. MATERIALS AND METHODS

2.1. Study area

The experimental field was located at "La Conchuela" farm, Córdoba, Spain (37°48′N, 4°48′W) at 147 m above sea level. The olive orchard was planted in 1993 with trees at 6 × 7 m spacing (238 tree ha^{-1}). Fig. 1 shows six of the eight plots selected for the ground measurements. They were selected to ensure a gradient in fraction of vegetation cover, ranging between 30% and 60%. The study sites comprised a range of crown leaf area densities (LAD) ranging from 0.45 to 1.02, tree heights between 3.5 and 5.2 m, and horizontal crown radii between 1.8 and 2.9 m (Fig. 1, Table 1). The field campaign was conducted in September, 2008. The ground measurements were conducted on the selected plots coincident with the airborne flight campaigns.

2.2 Ground and remote sensing airborne campaigns

Field campaigns were conducted for both airborne imagery acquisition and intercepted PAR field measurements collected, to asses the effects of the variability of the intercepted solar radiation and reflectance bands

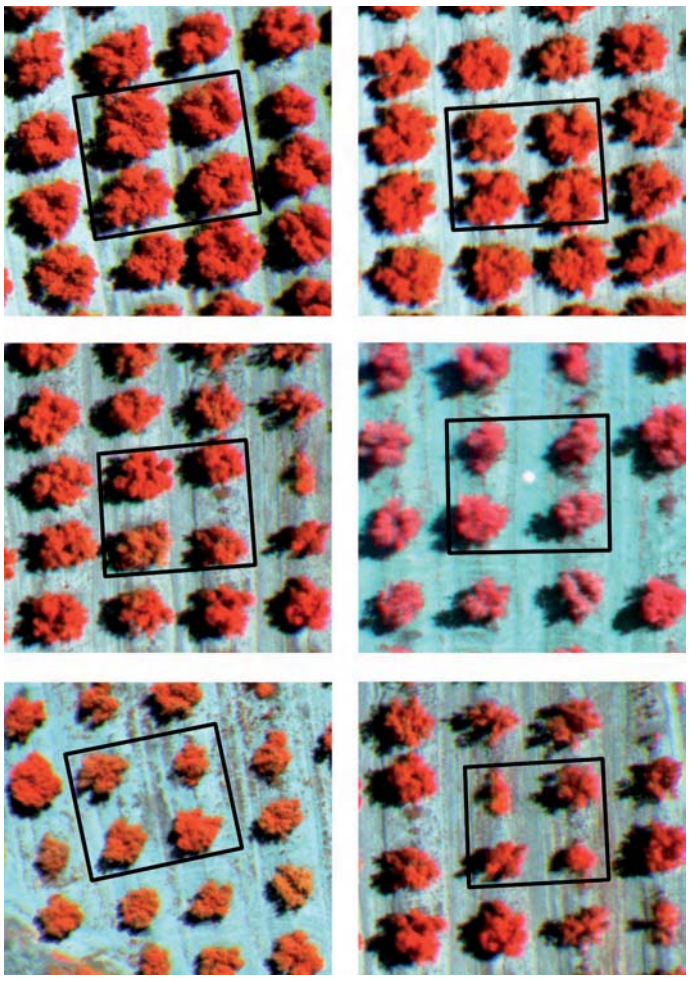

Fig. 1. Multispectral reflectance images acquired at 10 nm FWHM and 15 cm spatial resolution, showing six study plots used in the study. The central block area of 4 trees selected on each study site for field data collection is shown.

Table 1
Structural data collected from each study area

Stand	Crown radius (m)	Tree height (m)	LAD (m^2m^{-3})	LAI (m^2m^{-2})	Fraction of vegetation fraction (%)
1	2.3	4.4	0.54	0.57	39.5
2	1.8	3.5	1.02	0.6	24.2
3	2.9	5.2	0.43	0.9	63
4	2.0	4.1	0.62	0.5	30
5	2.8	4.9	0.45	0.8	58.6
6	2.1	3.8	0.97	0.9	33
7	2.5	4.0	0.56	0.7	46.7
8	2.3	4.0	0.54	0.6	39.5

Planting grid: 7 × 6 m. LAD—Leaf area density; LAI—Leaf area index.

as a function of orchard architecture. The interception of solar radiation by the orchard canopy on each study site was measured with a ceptometer (SunScan Canopy Analysis System, Delta-T Devices Ltd., Cambridge, UK). The instrument comprises two units: (i) a portable probe, 1 m long, for measuring the transmitted photosynthetically active radiation (PAR) flux beneath the canopy; and (ii) a beam fraction sensor (BFS) that measures PAR incident over the canopy at the same time. The BFS unit incorporates two photodiodes, one of which can be shaded from the direct solar beam by a shade ring. This allows the direct and diffuse components of PAR to be separated, since the fraction of the intercepted PAR by a tree is influenced by the rest of the surrounding trees and background. Therefore, the area comprising the 4 central trees of each study area was selected to conduct the field measurements of fIPAR. The measurements of transmitted PAR made in the area beneath the four central trees of each plot were in a 1 × 0.5 m grid. A schematic view is shown in Fig. 2a, and the actual measurements for two study areas are depicted in Fig. 2b. For the assessment of the spatial variation of fIPAR among the different selected plots with a gradient in structural parameters, measurements were conducted at 10:00 GMT (+/–half-hour).

Additional ground-level efforts were made to collect in situ measurements of crown structure, and leaf and soil optical properties, to characterize the different study plots and to use as input for the models. Dimensional properties, namely crown height and crown width, were measured at multiple points within a given olive tree. The crown was divided into eight sections; in each one the tree silhouette was estimated by measuring the upper and lower limits of the canopy with a vertical scaled pole that was systematically moved outward from the tree center in 0.2 m increments (Villalobos et al., 1995). In addition to in situ measurements of crown dimensions, the LAI-2000 Plant Canopy Analyzer (PCA) was used to estimate leaf area index at the individual crown level, as shown in Villalobos et al. (1995), and more recently Moorthy et al. (2011) and Gómez et al. (2011). This device measures the fraction of diffuse incident radiation transmitted through a plant canopy by calculating the ratio of the below- and above-canopy radiation measurements. It has a set of optical sensors that simultaneously measure diffuse radiation in five ranges of zenith angles (this methodology is described in detail in Gómez et al., 2011). The leaf angle distribution functions used was the ones measured by Mariscal et al. (2000) in adult trees (Fig. 3).

The multispectral sensor used in this study was a 6-band multispectral camera (MCA-6, Tetracam Inc., California, USA). The camera consists of 6 independent image sensors and optics with user-configurable spectral filters. The image resolution is 1280 × 1024 pixels with 10-bit radiometric resolution and optics focal length of 8.5 mm, yielding an angular field of view (FOV) of 42.8º × 34.7º and 15-cm pixel spatial resolution at 150-m flight altitude. High-resolution multispectral images acquired over the olive orchards enabled the identification of each study site used for field measurements of crop structure and fIPAR. The plots were marked in the field using bright ground control points easily detectable on the imagery. The bandsets selected for this study comprised center wavelengths at 670 and 800 nm with 10 nm full width at half maximum (FWHM) used for computing the *Normalized Difference Vegetation Index* (NDVI). Figure 1 shows the imagery acquired by the multispectral airborne sensor at 15 cm spatial resolution, representing six fields used in this study with a range in fraction of vegetation cover, and the block of 4 trees selected on each study site for field data collection of radiation interception. The high spatial resolution acquired enabled targeting pure scene

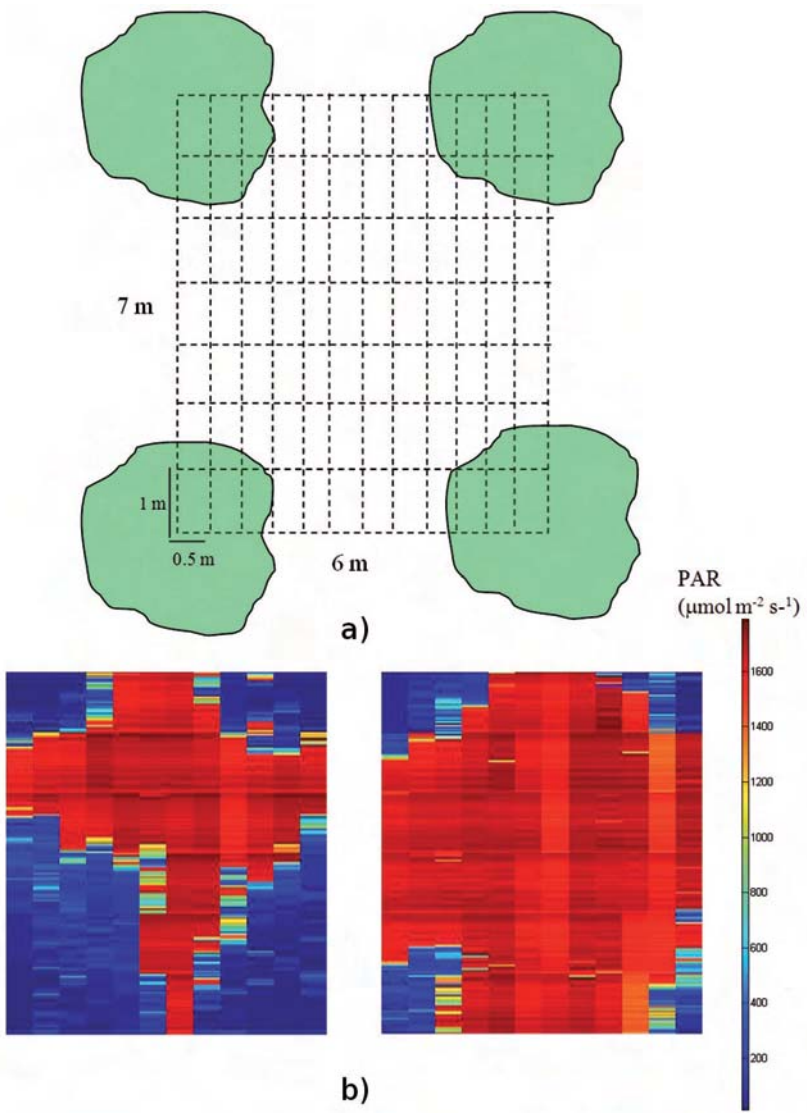

Fig. 2. Schematic view of the 1× 0.5 m grid used for field measurements conducted with the ceptometer (a); (b) PAR data measured by ceptometer at the ground level.

components, such as pure soil and vegetation, separately as well as on aggregated pixels. Atmospheric correction and radiometric calibration methods were applied to the imagery to calculate the spectral reflectance. Radiometric calibration was conducted in the laboratory using coefficients derived from measurements made with a uniform calibration body (integrating sphere, CSTM-USS-2000C Uniform Source System, LabSphere, NH, USA) at four levels of illumination and eleven integration times. Radiance values were converted to reflectance using the total incoming irradiance simulated with the Simple Model of the Atmospheric Radiative Transfer of Sunshine (SMARTS) (Gueymard, 1995, 2005) using aerosol optical depth at 550 nm measured with Micro-Tops II sunphotometer (Solar LIGHT Co., Philadelphia, PA, USA). This radiative transfer model was previously used in other studies such as Berni et al. (2009) and Suárez et al. (2010). The geometric calibration was conducted using Bouguet's calibration method (Bouguet, 2001) in order to calculate the intrinsic camera parameters (Berni et al., 2009).

Leaf optical properties, and their reflectance and transmittance measurements, were acquired on leaf samples using an Integrating Sphere (Li-Cor 1800-12, Inc., Lincoln, NE, USA), coupled with a 200-μm diameter single mode fiber to a spectrometer (Ocean Optics Inc. model USB2000, Dunedin, FL, USA), with a 1024-element detector array, 0.5 nm sampling interval, and

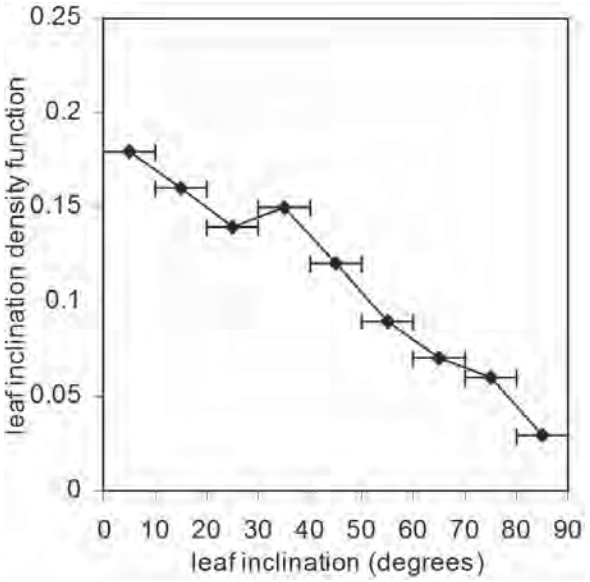

Fig. 3. Leaf angle distribution function in 10º intervals, measured for olive adults trees (Mariscal et al., 2000).

7.5 nm spectral resolution in the 340–940 nm range. The single leaf values for reflectance (ρ) and transmittance (τ) were acquired as described in the manual of the Li-Cor 1800-12 system (Li-Cor, 1983) and in Zarco-Tejada et al. (2005), using a custom-made port of 0.5 cm diameter suited to typical olive leaf dimensions and thereby obtaining the leaf optical properties. A total of 300 leaves were sampled. Figure 4a shows the mean leaf reflectance and transmittance measured on olive leaves. The spectral range for the leaf optical properties used as input for the models was selected according to the bandset used in the airborne imagery (Fig. 4b). Sunlit soil reflectance was extracted from the airborne imagery (Fig. 5).

Table 1 and Figs. 3, 4, and 5 show the field measurements collected on each study site. They will be used as inputs for the 3D canopy modelling work conducted with FLIGHT on the aggregated reflectance and fIPAR estimation, as well as for the ORIM model to estimate fIPAR in olive orchards. Table 2 shows the input parameters required by these models.

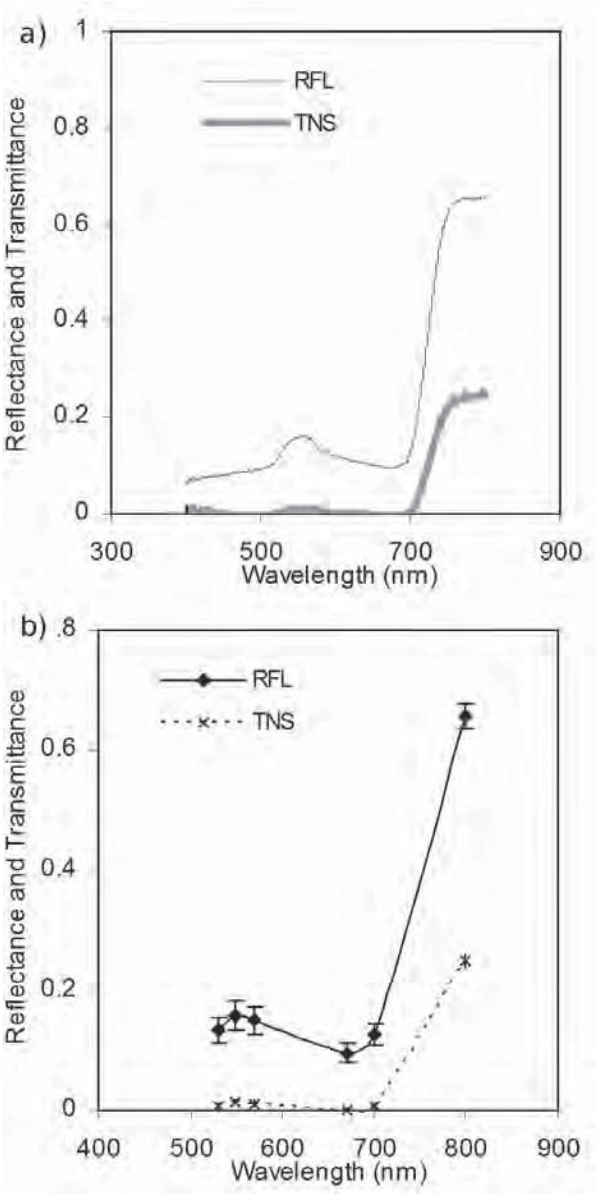

Fig. 4. (a) Reflectance and transmittance spectra measured by integrating sphere for olive leaves; (b) reflectance and transmittance spectra for the olive leaves with the bandset used in this study.

2.4. fIPAR estimation in olive orchards from remote sensing data

2.4.1. FLIGHT and ORIM models for simulating fIPAR in olive orchards

Two models are proposed in this manuscript to estimate fIPAR in olive orchards: a 3D model of light interaction with vegetation canopies FLIGHT (North, 1996), and the ORIM model of PAR interception by olive canopies as formulated by Mariscal et al. (2000). The FLIGHT model is based on the Monte Carlo ray tracing method as a tool to simulate the radiative transfer in a canopy structure (North, 1996). Monte Carlo simulation allows highly accurate estimation of light interception and bidirectional reflectance (Disney et al., 2000; Barton and North, 2001). In the FLIGHT model, an accurate treatment of the light interception and multiple scattering between foliage elements and soil boundary is obtained by iteration (North, 2002).

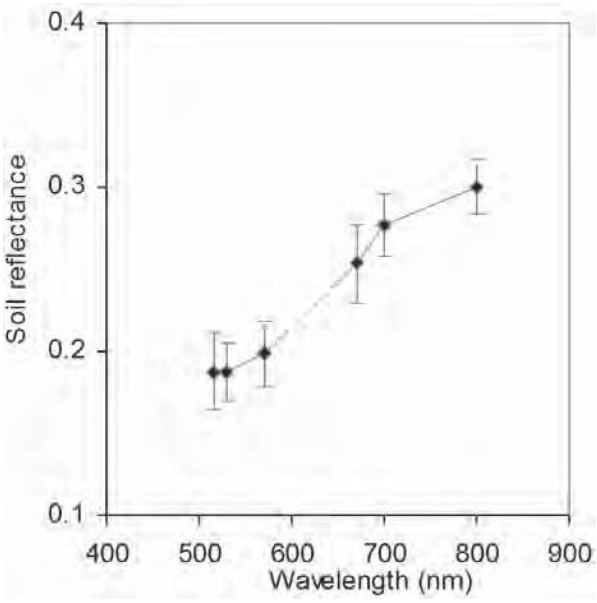

Fig. 5. Soil optical properties of the study area.

The FLIGHT model has been assessed with other three-dimensional codes as part of the *Radiation Model Intercomparison* (RAMI) project (Wildowski et al., 2007). The recent analysis conducted within RAMI on six selected three-dimensional models, including FLIGHT, showed dispersion within 1% over a large range of canopy descriptions (Wildwoski et al., 2008). In this study, FLIGHT was selected because it allowed the simulation of planting grids, tree dimensions, and soil background effects, making it easy to generate several 3D scenes for the assessment of the effects of the architecture, crown structure and biochemical inputs. This model has been previously used in other work simulating row-orientated orchards, such as orange and peach, with successful results (Suárez et al., 2009; Suárez et al., 2010; Guillén-Climent et al., 2012). The FLIGHT model inputs consist of: (i) geometric characteristics, (ii) optical properties, (iii) sun and view azimuth and zenith angles, and (iv) other parameters such as soil roughness, aerosol optical thickness and the number of photons simulated. Table 2 shows the input parameters required to run the model. The output of FLIGHT is a 3D hyperspectral image and the estimated intercepted PA (*IPAR*) for the scene.

The ORIM model is reliable for estimating radiation intercepted by any olive orchard at instantaneous and daily levels (Mariscal et al., 2000). The model works at an hourly time step, integrating the radiation reaching a convenient number of spatial cells. It was later modified to obtain a simplified PAR interception model for practical purposes, with daily time steps (Orgaz et al., 2007). This model allows simulating row orientation, tree dimensions, and slope of the field. It has been used by Iniesta et al. (2009) and Fernandes-Silva et al. (2010), among others, to estimate the amount of annual IPAR. The inputs required by ORIM are the planting pattern, row and column angles, soil PAR reflectance, latitude, height, tree perpendicular radii of the crown, and leaf area density (LAD) (Table 2). Leaf reflectance and transmittance, and *G-function* are internal parameters calculated for olive trees. ORIM model outputs are estimations of all the components of the radiation balance for hourly, daily, and seasonal periods.

A detailed simulation of fIPAR was undertaken to assess the performance of both the FLIGHT and ORIM models for this type of olive canopy. The study areas were simulated using the structural and optical measurements collected at each plot (see Figs. 3, 4, and 5 for leaf angle distribution function and the leaf and soil optical properties, and Table 1 for the structural measurements used). Model assessment for the fIPAR simulations was conducted by comparing the modelled fIPAR obtained from each model against the ceptometer measurements acquired on each plot, calculating the RMSE obtained. Once the two models were assessed for fIPAR estimation from field datasets, a second step consisted of testing each model for fIPAR estimation on all plots from the airborne remote sensing imagery acquired. This second assessment was carried out with predictive relationships developed between NDVI and fIPAR obtained through modelling. Two methods were used: (i) obtaining the canopy reflectance and fIPAR from FLIGHT; (ii) using simulated canopy reflectance from FLIGHT coupled with the ORIM model (FLIGHT + ORIM). In this way, FLIGHT and ORIM models were assessed for their capability to estimate fIPAR both from field data and airborne imagery (Fig. 6). The aggregated image reflectance from the four central trees of the orchard, including exposed soil and shadows, was used to compute spectral vegetation indices, such as NDVI.

Previous to the estimation of fIPAR using airborne remote sensing imagery, a study was carried out with modelling methods to understand the influence of the architecture of the canopy on aggregated NDVI and fIPAR. The fraction of vegetation cover was varied from 20 to 60% for three different solar angles (solar zeniths 70.9º, 35.02º, and 29.6º), and two types of soil reflectance spectra were used to study their effects on NDVI and fIPAR.

2.4.2. fIPAR estimation from remote sensing imagery using modelling methods

Relationships between NDVI and fIPAR were developed to estimate the instantaneous fIPAR in the olive orchards using the airborne imagery acquired on each

Table 2
Nominal values and range of parameters used for canopy modelling with FLIGHT and ORIM models

FLIGHT model—Input parameters	Values/Unit used
Leaf optical and structural parameters	
Hemispherical reflectance and transmittance of green leaves	integrating sphere
Hemispherical reflectance and transmittance of senescent leaves	not used
Leaf equivalent radius	m
Canopy layer and structural parameters	
Leaf area index of vegetation	See Table 1
Fractional cover	30–60%
Leaf angle distribution function	Empirical
Fraction green leaves	1
Fraction senescent leaves	0
Fraction of bark	0
Hemispherical reflectance and transmittance of bark	Not used
Number of stands and position coordinates	Coord. (m)
Crown shape	Elliptical
Crown height and radius	m (see Table 1)
Trunk height and radius	m (see Table 1)
Background and viewing imagery geometry	
Solar zenith and azimuth angles	Degrees
Sensor zenith and azimuth angles	Degrees
Soil reflectance	From image
Soil roughness	0
Aerosol optical depth (AOD)	0.15
ORIM model—Input parameters	**Values /Unit used**
Crown height and radius	m
Planting pattern	m x m
LAD (leaf area density)	$m^2\ m^{-3}$
Row and column angles	Degrees
Soil PAR reflectance	From image
Latitude	37.8° N
Internal parameters	
G-function	measured (Mariscal et al., 2000)
Leaf reflectance and transmittance	measured (Mariscal et al., 2000)

study site using pixels that integrated each study site. In particular, the objective was to develop predictive relationships NDVI–fIPAR calculated under specific canopy assumptions valid for the study sites under study. These relationships were obtained (i) with FLIGHT; (ii) with the canopy reflectance module from FLIGHT linked to the ORIM fIPAR estimation model (Fig. 6).

The fIPAR predictive relationships for the olive canopies were developed with input parameters fixed according to mean field measurements: leaf angle distribution function, leaf optical properties, planting grid and soil reflectance extracted from the airborne image, and the solar geometry depending on the time of flight. The specific input parameters varied within the typical range of variation for these orchards to account for the canopy structure were 0.5 to 3 m in the case of crown radii, tree height ranged from 2 to 6 m, and LAI from 0.1 to 1 (Table 3). The modeled relationships NDVI vs. fIPAR obtained for each study plot were then applied to the multispectral airborne imagery reflectance to estimate the instantaneous fIPAR for each study site. Relationships were obtained for the olive orchard with both model approaches: (i) FLIGHT; and (ii) FLIGHT + ORIM (Fig. 6). This methodology enabled the application of sensor-derived optical indices for NDVI–fIPAR that are a function of canopy structure, optical properties, and the viewing geometry. Relationships between vegetation indices and fIPAR have been suggested in

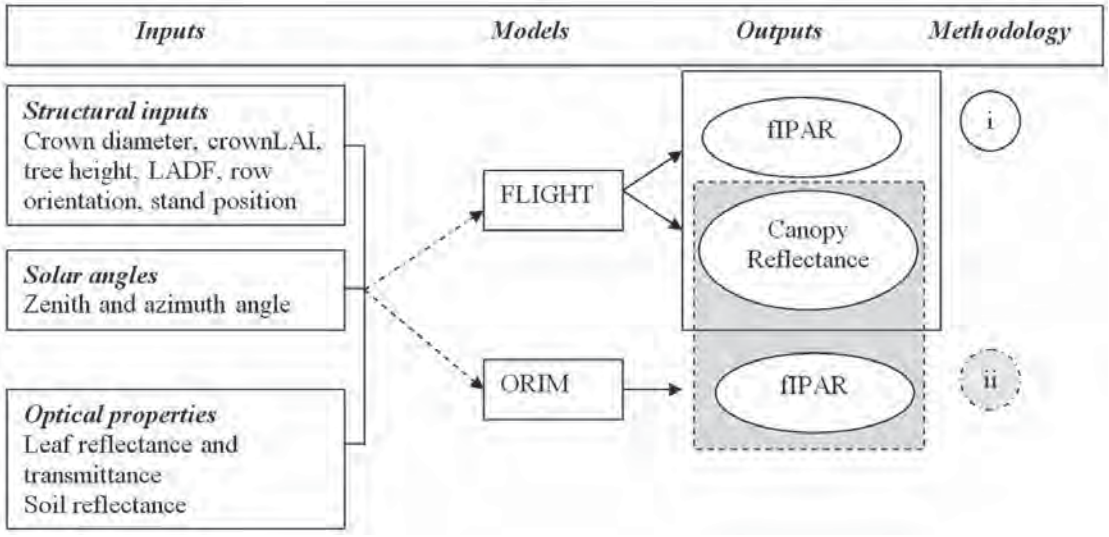

Fig. 6. Schematic view of the coupling method between FLIGHT and ORIM models to develop predictive relationships between NDVI and fIPAR.

Table 3
Input parameters used to generate predictive fIPAR-NDVI algorithms. Determination coefficients and RMSE values obtained between the ground-measured fIPAR and the estimated fIPAR from FLIGHT and FLIGHT + ORIM

Parameter	Source/Value
Fixed parameters	
LADF	Measured (Fig. 3)
Leaf (ρ and τ)	Measured (Fig. 4b)
Row orientation	63º from North
Sun geometry	SZ:35.02º; SA:69.5º
Soil (ρ_s)	Obtained from image (Fig. 5)
Variable parameters	
Tree radius (m)	0.5–3
Tree height (m)	2–6
LAI	0.1–1
Results	r^2 ;(RMSE)
FLIGHT	0.85; 0.11
FLIGHT + ORIM	0.83; 0.05

LADF—Leaf angle distribution function; SZ—solar zenith (degrees from the vertical); SA—solar azimuth (degrees from South, clockwise negative); LAI—Leaf area index.

previous works, mainly in studies dedicated to herbaceous crop or forest canopy. To assess the behaviour on heterogeneous open-tree orchards of these relationships originally developed for homogeneous canopies, a relationship by Myneni and Williams (1994) (fAPAR = 1.1638*NDVI–0.1426) was applied to the study plots selected on this work, and the error obtained was calculated.

3. RESULTS

3.1 Results for fIPAR estimation from FLIGHT and ORIM models

The simulations corresponding with the different study plots in the olive orchard were assessed with both models to evaluate the correspondence of the simulations with fIPAR field measurements. Figure 7 illustrates four scenarios corresponding to four different study plots in the olive orchard. Error assessments conducted for fIPAR estimated with FLIGHT and ORIM models using ceptometer field data are shown in Figs. 8a and 8b, respectively. The estimation of fIPAR yielded RMSE = 0.10 with coefficient of determination of $r^2 = 0.5$ when using FLIGHT, and RMSE = 0.05, $r^2 = 0.81$ for ORIM simulations. The ORIM model therefore yielded better results than FLIGHT for simulating fIPAR from field-measured architectural and structural parameters in olive canopies. The simulations conducted with FLIGHT and ORIM models to assess the sensitivity of the input parameters, such as fraction of vegetation cover, sun angles, and the soil reflectance on NDVI and fIPAR, were investigated generating canopy scenarios (Fig. 9a for NDVI, and Fig. 9b for fIPAR). Figures 9a and 9b show the effect of soil optical properties on the aggregated NDVI to be greater than in fIPAR estimates. In scenes with 60% vegetation cover and solar zenith angle 35.02º, NDVI varied from 0.53 for a dark soil to 0.43 for a bright soil, while fIPAR for the same canopy scenario changed only from 0.50 to 0.48. The large soil reflectance variation mainly affects the NDVI vs. fIPAR relationship as a function of the background. The solar

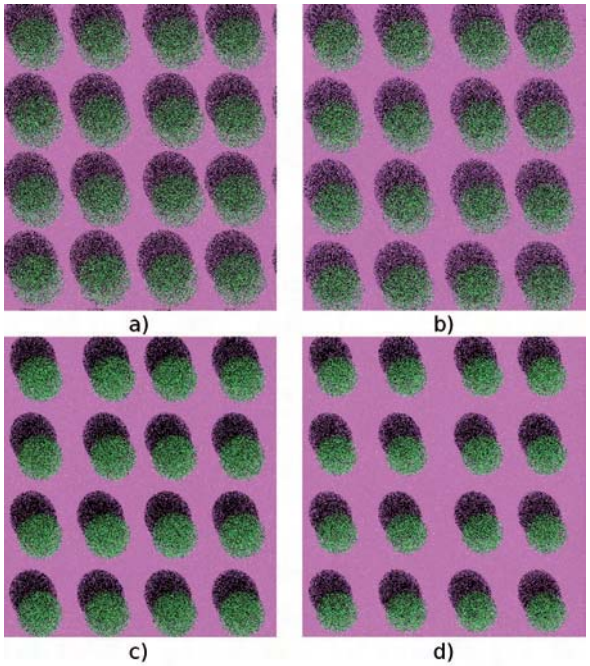

Fig. 7. Model simulations conducted with FLIGHT to generate orchard scenes for different fractions of vegetation cover. Input parameters used were the aerosol optical thickness (0.15), solar zenith (35.02º), solar azimuth (69.5º, East = 0º), view zenith and azimuth angles (0º). Architectural properties correspond with study areas described in Table 1: stand 5 (a), stand 7 (b), stand 6 (c) and stand 2 (d).

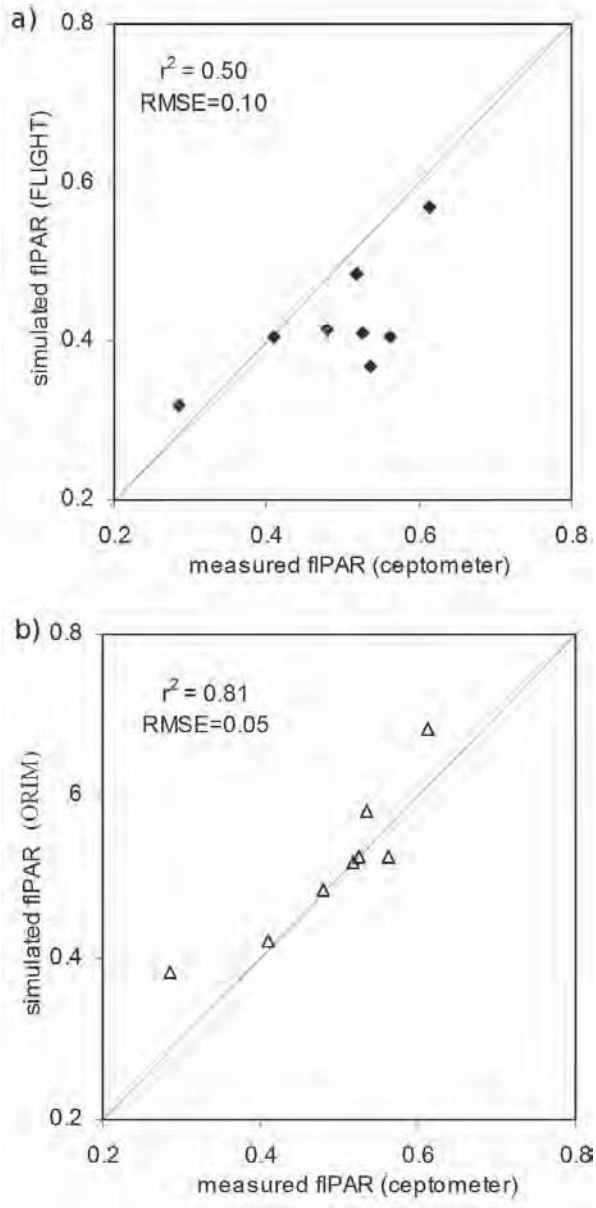

Fig. 8. Relationships between fIPAR ground measurements and fIPAR estimations using FLIGHT (a) and ORIM (b). The input parameters used for both models were the ground measurements collected at each study site (Table 1, Fig. 3).

angle showed to have effects on both fIPAR and NDVI, as expected. For a north–south rectangular planting grid orchard, the intercepted PAR was higher at high zenith angles: fIPAR varied from 0.7 in the morning (SZ = 70.9º) to 0.4 at midday (SZ = 35.02º) for a 60% vegetation cover and dark soil (Fig. 9b). The differences found in NDVI for different solar angles were caused also by the soil reflectance and the amount of shadow; nevertheless, the effect was smaller than in fIPAR. NDVI varied from 0.5 to 0.4 for a 60% vegetation cover and dark soil, and from 0.62 to 0.48 for a bright soil (Fig. 9a). The study showed that NDVI vs. fIPAR relationships cannot be readily applied to open canopy orchards due to the large effects caused by parameters such as soil reflectance and sun angle, and appropriate modelling techniques are needed to develop accurate relationships for the fIPAR estimation in these orchards.

3.2. Estimating fIPAR using FLIGHT and the coupled FLIGHT+ORIM model

An analysis on fIPAR estimation with remote sensing imagery was conducted by developing relationships between vegetation indices calculated from the airborne imagery and fIPAR measured with a ceptometer (Fig. 10). The variation of NDVI vs. fIPAR (Fig. 10) was obtained through measurements conducted at selected plots with different architectural canopy characteristics at 10:00 GMT (+/–half hour). The results showed high coefficient of determination for NDVI vs. fIPAR with $r^2 > 0.9$ for a polynomial regression.

The modeled relationships NDVI vs. fIPAR were

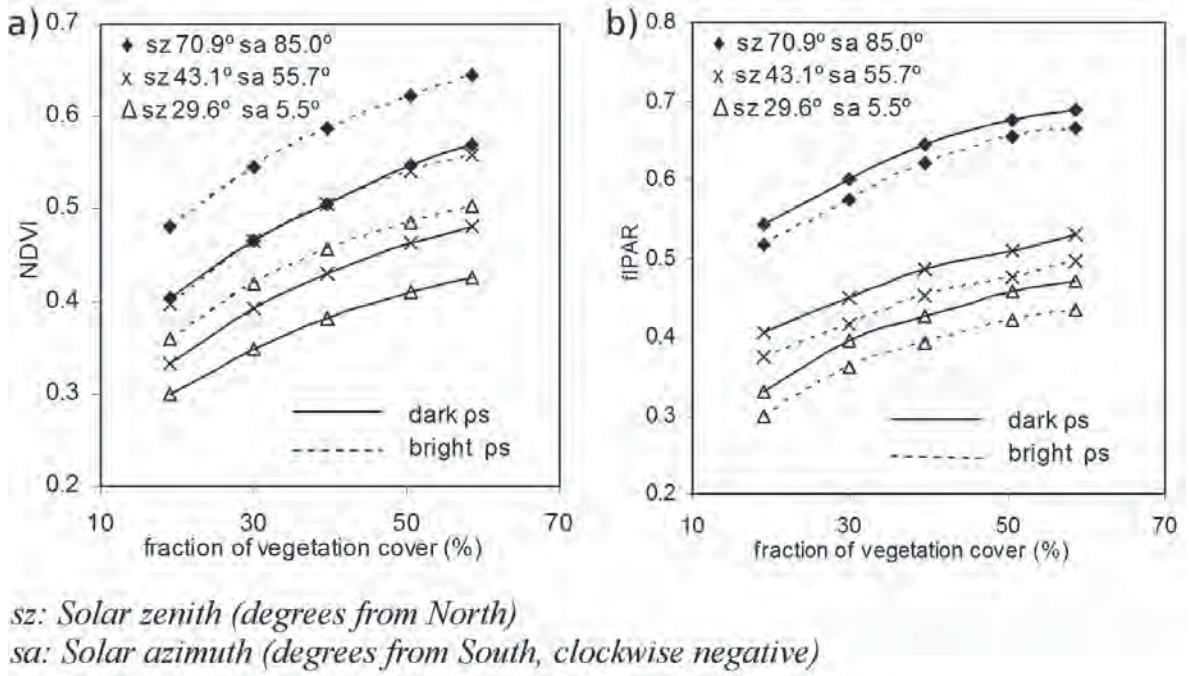

Fig. 9. Variance analysis to study the effect of the sun geometry, soil optical properties and fraction of vegetation cover on NDVI (a) and fIPAR (b) using the FLIGHT model. It was considered row orientation N–S, LAI = 0.8, leaf size = 0.0075, fraction of green leaves = 1.0, fraction of bark = 0, LADF defined by user, ellipsoidal crown shape, soil roughness = 0, and aerosol optical thickness = 0.1.

obtained with the FLIGHT model (Fig. 11a) and with the FLIGHT and ORIM models (Fig. 11b). Input parameters were field-measured, while the inputs related to canopy architecture were ranged within the typical range of variation for these orchard crops (see Table 3). Relationships obtained for the olive orchard with both models—(i) FLIGHT, and (ii) FLIGHT + ORIM (Fig. 6)—yielded slightly different results, showing better agreements with the FLIGHT + ORIM coupled simulation model (Fig. 11b). Estimation of fIPAR by predictive relationships was compared against ground measured fIPAR for each plot. The fIPAR output from FLIGHT was slightly underestimated when compared against FLIGHT + ORIM. Relationships obtained for the orchard yielded fIPAR estimates with relative RMSE of 0.11 and $r^2 = 0.85$ when FLIGHT was used, and RMSE = 0.05 and $r^2 = 0.83$ for FLIGHT + ORIM coupled models

The assessment of the Myneni and Williams (1994) relationship developed for homogeneous crop (fAPAR = 1.1638 * NDVI – 0.1426), when applied to the study plots selected for this work, yielded an error of RMSE = 0.24. This result demonstrates that higher errors were

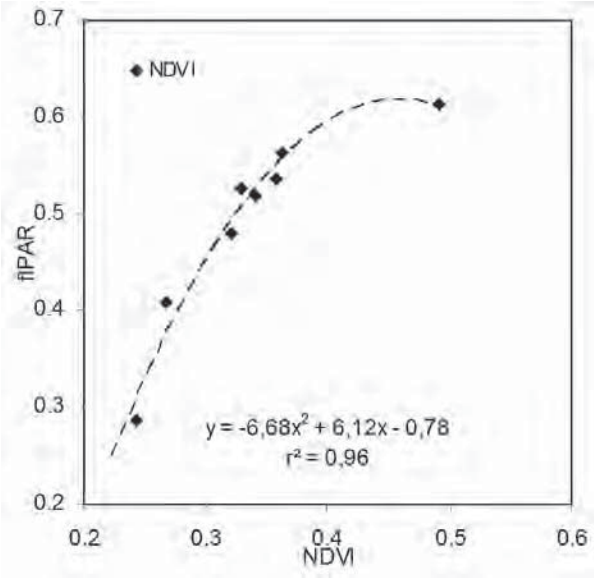

Fig. 10. Relationships between airborne imagery NDVI and field-measured fIPAR for the eight study sites imaged at solar zenith angle = 35.02º.

obtained in their work as compared to our FLIGHT (RMSE = 0.11) and FLIGHT + ORIM (RMSE = 0.05) simulations (Fig. 12).

Finally, a high-resolution multispectral mosaic acquired over one of the study areas (Fig. 13a) was used to generate a map of the spatial variability of the radiation interception. The map was generated following the methodology described in this paper. The aggregated reflectance and NDVI was calculated from a grid, each comprised of four trees, shadows, and soil. The FLIGHT + ORIM predictive relationships were then applied to the grid NDVI scene of the olive orchard, generating a map of the spatial variability of the instantaneous fIPAR (Fig. 13b).

4. CONCLUSIONS

A remote sensing study focused on estimating fIPAR on olive tree canopies was conducted. This work investigated the relationship between canopy reflectance and instantaneous fIPAR in olive orchards, using radiative transfer modelling methods and field measurements. The PAR intercepted by the orchard canopy was simulated through two approaches: (i) using the FLIGHT

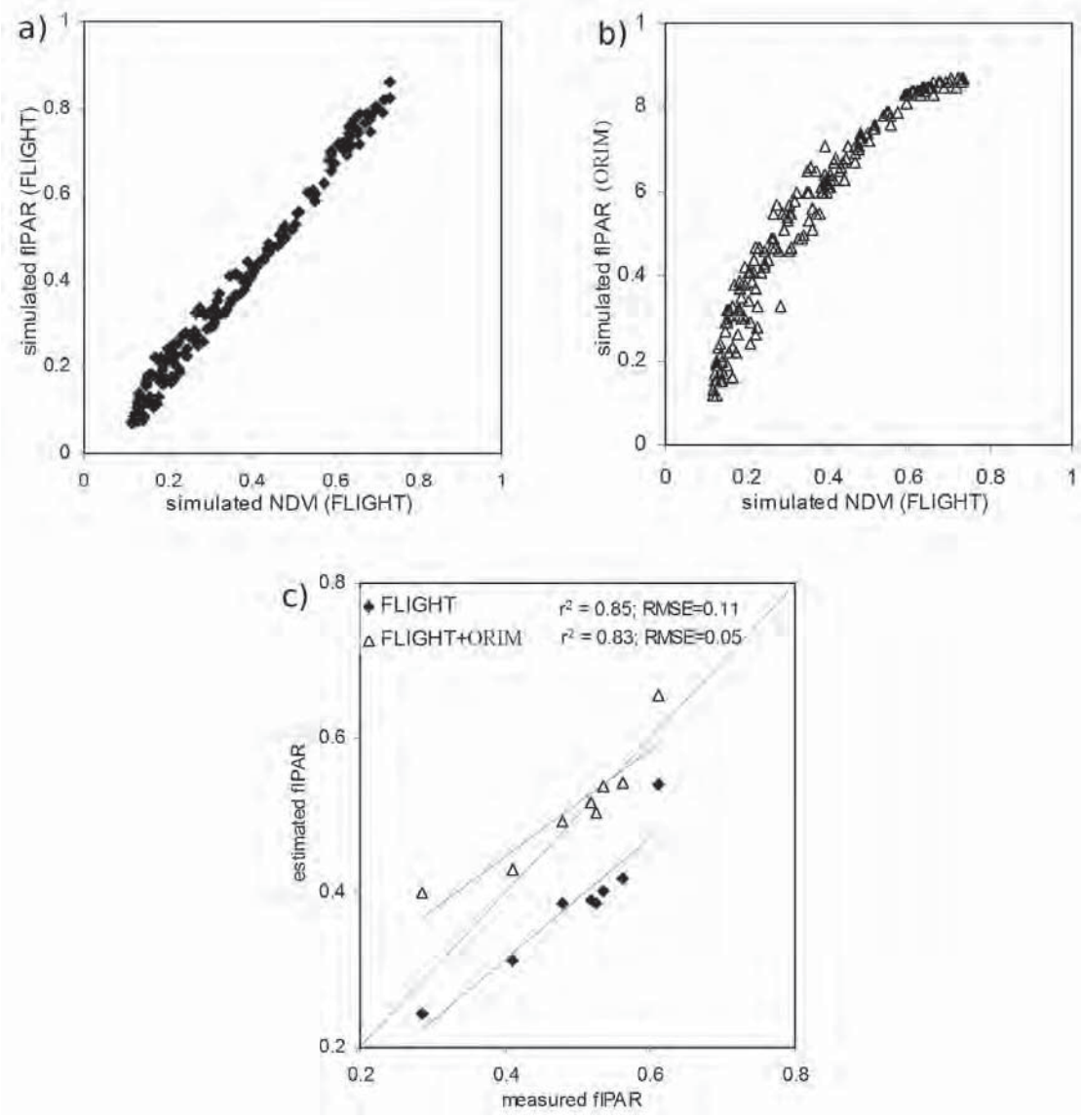

Fig. 11. Predictive relationships obtained between NDVI and fIPAR from FLIGHT (a) and FLIGHT + ORIM (b) for olive orchards. Estimated fIPAR using predictive relationships developed in (a) and (b) versus measured fIPAR (c).

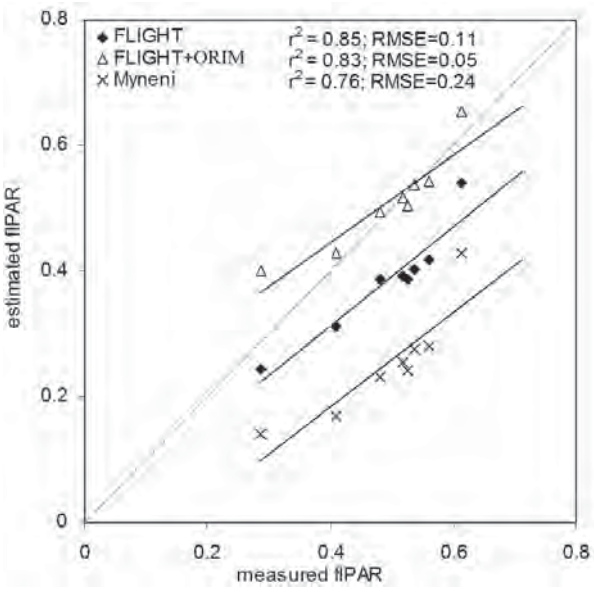

Fig. 12. Estimated fIPAR using the predictive relationships developed in this manuscript vs. that published for homogeneous crops (Myneni and Williams, 1994).

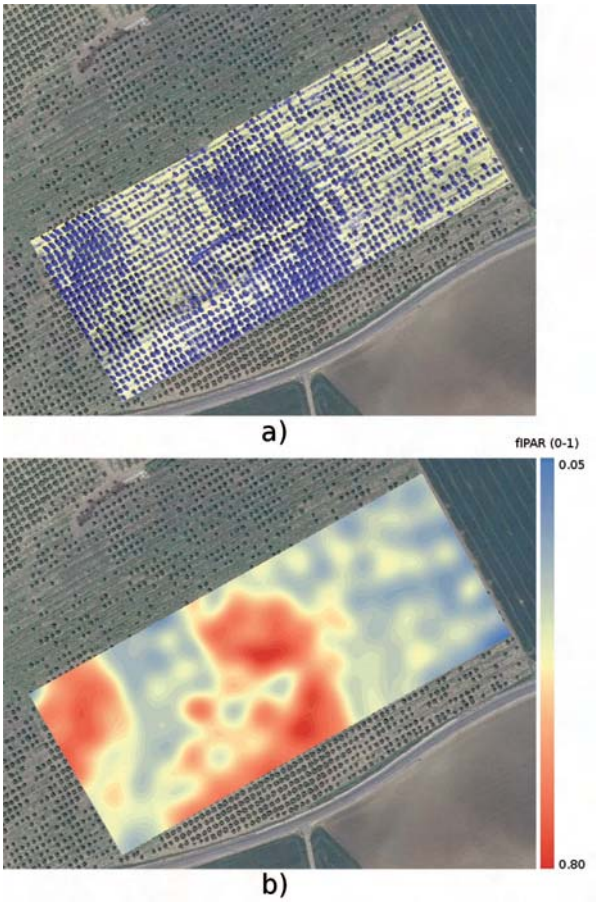

Fig. 13. Multispectral mosaic of the olive orchard (a) used to generate a map of fIPAR calculated from the coupled FLIGHT + ORIM model (b) using the methodologies described in this manuscript.

3D model; and (ii) using a specific simulation approach to estimate fIPAR in olive orchards, ORIM model. Both models were firstly assessed using input parameters measured in the field at different study plots. The FLIGHT model yielded a RMSE of 0.1 for fIPAR, while the ORIM model obtained better results, with an RMSE of 0.05 when compared against fIPAR ground-measured data. In conclusion, these results demonstrated better fIPAR estimates when using the ORIM model and ground data collected over the study sites used for the model assessment. In addition, this study examined the effect of varying background optical properties, sun angles, and fraction of vegetation cover on fIPAR and NDVI index when aggregating the canopy reflectance from the four central trees of the simulated scenes. The NDVI–fIPAR relationships were showed not to be applicable to all canopy types due to the important effects caused by soil and shadows. A set of simulations conducted on two scenes with varying soil reflectance results showed important effects on NDVI, with an almost negligible influence on fIPAR. In such set of simulations, NDVI varied from 0.35 to 0.45 for two different soil types, while fIPAR changed from 0.37 to 0.39 for the same fraction of vegetation cover and solar angles, due only to the different soils backgrounds. In conclusion, the NDVI vs. fIPAR relationship is critically affected by the soil optical properties in such open tree orchards, requiring the use of radiative transfer models for an accurate estimation of fIPAR in olive canopies.

The results obtained from predictive NDVI–fIPAR relationships showed that FLIGHT + ORIM estimates were more accurate than the results obtained with FLIGHT alone. The trend showed a polynomial relationship between NDVI and fIPAR when FLIGHT + ORIM couple model was used, while FLIGHT showed a linear trend. The application of the predictive algorithms for fIPAR estimation yielded a relative RMSE of 0.11 (r^2 = 0.85) for FLIGHT model, and a RMSE of 0.05 (r^2 = 0.83) for the coupled FLIGHT + ORIM models. Although FLIGHT performed well for fIPAR estimation, the ORIM model showed superior performance. The ORIM model was formulated, calibrated, and validated specifically for olive orchards.

The methodology presented demonstrates the feasibility for estimating the spatial distribution of the instantaneous fIPAR in complex non-homogeneous orchard canopies. As expected, the use of NDVI–fIPAR

relationships obtained in previous works for homogeneous canopies yielded a higher error, with RMSE = 0.24. Thus, the particularities of the different type of canopies need to be accounted for when estimating fIPAR and others biophysical parameters. Further work will focus on other plant-grid plantations, such as the current intensive olive plantations, including diurnal studies to investigate the variability and uncertainties associated with these methodologies. In addition, the estimation of daily PAR interception from estimated instantaneous fIPAR on these non-homogeneous complex canopies will be assessed. Obtaining maps of the spatial variability of fIPAR may provide valuable information for decision makers to design new plantations according to water availability and crop potential.

ACKNOWLEDGMENTS

Financial support from the Spanish Ministry of Science and Innovation (MICINN) for projects AGL2009-13105, CONSOLIDER CSD2006-67, and AGL2003-01468 is gratefully acknowledged, as well as the Junta de Andalucía-Excelencia AGR-595 and FEDER. M.L. Guillén-Climent was supported by a JAE grant of CSIC, co-funded by the European Social Fund. P.R.J. North is gratefully acknowledged for sharing the FLIGHT code. The members of the QuantaLab-IAS-CSIC are acknowledged for scientific and technical support in field and airborne campaigns.

REFERENCES

Annandale, J.G., Jovanovic, N.Z., Campbell, G.S., Du Sautoy, N., Lobit, P. 2004. Two-dimensional solar radiation interception model for hedgerow fruit trees. Agr. Forest. Meteorol. 121: 207–225.

Asrar, G., Fuchs, M., Kanemasu, E.T., Hatfield, J.H. 1984. Estimating absorbed photosynthetic radiation and leaf area index from spectral reflectance in wheat. Agron. J. 76: 300–306.

Barton, C.V.M., North, P.R.J. 2001. Remote sensing of canopy light use efficiency using the photochemical reflectance index. Model and sensitivity analysis. Remote Sens. Environ., 78: 264–273.

Beede, R.H., Goldhamer, D.A. 1994. Olive irrigation management In: Ferguson, L., Sibbett, G.S., Martin, G.C. eds. Olive production manual. Univ. of California Pub. 3353, pp. 61–68.

Ben-Gal, A., Yermiyahu, U., Zipori, I., Presnov, E., Hanoch, E., Dag, A. 2011. The influence of bearing cycles on olive oil production response to irrigation. Irrig. Sci. 29: 253–263.

Berni, J.A.J., Zarco-Tejada, P.J., Suarez, L., Fereres, E. 2009. Thermal and narrow-band multispectral remote sensing for vegetation monitoring from an unmanned aerial vehicle. IEEE Trans. Geosci. Electron. 47: 722–738.

Bouguet, J. 2001. Camera calibration toolbox for Matlab. (http://www.vision.caltech.edu/bouguetj/calibdoc/index.html).

Connor, D.J., Fereres, E. 2005. The physiology of adaptation and yield expression in olive. Horicultural Reviews 31: 155–229.

Daughtry, C.S.T., Gallo, K.P., Bauer, M.E. 1983. Spectral estimates of solar radiation by corn canopies. Agron. J. 75: 527–531.

De Castro, F., Fetcher, N. 1998. Three dimensional model of the interception of light by a canopy. Agr. Forest. Meteorol. 90: 215–233.

Disney, M.I., Lewis, P., North, P. R. J. 2000. Monte Carlo ray tracing in optical canopy reflectance modelling. Remote Sens. Rev. 18: 163–196.

Fernades-Silva, A.A., Ferreira, T.C., Correia, C.M., Malheiro, A.C., Villalobos, F.J. 2010. Influence of different irrigation regimes on crop yield and water use efficiency of olive. Plant Soil 333: 35–47.

Friday, J.B., Fowness, J.H. 2001. A simulation model for hedgerow light interception and growth. Agr. Forest. Meteorol. 108: 29–43.

Gómez, J.A., Zarco-Tejada, P.J., García-Morillo, J., Gama, J., Soriano, M.A. 2011. Determining biophysical parameters for olive trees using CASI airborne and Quickbird satellite imagery. Agron. J. 103: 644–654.

Gueymard, C.A. 1995. SMARTS, A Simple Model of the Atmospheric Radiative Transfer of Sunshine: algorithms and performance assessment. Technical Report No. FSEC-PF-270-95. Florida Solar Energy Center, Cocoa, FL.

Gueymard, C.A. 2005. Interdisciplinary applications of a versatile spectral solar irradiance model: a review. Energy 30: 1551–1576.

Guillen-Climent, M.L., Zarco-Tejada, P.J., Berni, J.A.J., North, P.R.J., Villalobos, F.J. 2012. rco-Tejada, P.J., Berni, J.A.J., North, P.R.J. and Villalobos, F.J. (2012), Mapping radiation interception in row-structured orchards using 3D simulation and high resolution airborne imagery acquired from a UAV. Precision Agriculture 13: 473–500.

Hall, F.G., Huemmrich, K.F., Goetz, S.J., Sellers, P.J., Nickerson, J.E. 1992. Satellite remote sensing of surface energy balance: success, failures, and unresolved issues in FIFE. J. Geophys. Res. 97: 19,061–19,089.

Huemmrich, K.F. 2001. The GeoSail model: a simple addition to the SAIL model to describe discontinuous canopy reflectance. Remote Sens. Environ. 75, 423-431.

Huemmrich, K.F. Goward, S.N., 1997. Vegetation canopy PAR absorptance and NDVI: an assessment for ten species with SAIL model. Remote Sens. Environ. 61: 254–269.

Iniesta F, Testi L, Orgaz F, Villalobos FJ. 2009. The effects of regulated and continuous eficit irrigation on the water use, growth and yield of olive trees. Eur. J. Agron. 30: 258–265.

Kempeneers, P., Zarco-Tejada, P. J., North, P. R. J., De Backer, S., Delalieux, S., Sepulcre-Cantó, G., Morales, F., Van Aardt, J. A. N., Sagardoy, R., Coppin, P., Scheunders, P. 2008. Model inversion for chlorophyll estimation in open

canopies from hyperspectral imagery. Int. J. Remote Sens. 29: 5093–5111.

Li-Cor Inc. 1983. 1800-12 Integrating Sphere instruction manual, Publication no. 8305-0034, Lincoln, NE USA.

Mariscal, M.J., Orgaz, F., Villalobos, F.J. 2000. Modelling and measurement of radiation interception by olive canopies. Agr. Forest. Meteorol. 100: 183–197.

Monteith J.L. 1977. Climate and the efficiency of crop production in Britain. Philos. Trans. R. Soc. London Ser. B 281: 277–294.

Moorthy, I., Miller, J.R., Berni, J.A.J., Zarco-Tejada, P.J., Hu, B., Chen, J. 2011. Field characterization of olive (*Olea europaea* L.) tree crown architecture using terrestrial laser scanning data. Agr. Forest. Meteorol. 151: 204–214.

Moriondo, M., Maselli, F., Bindi, M. 2007. A simple model of regional wheat yield based on NDVI data. Eur. J. Agron. 26: 266–274.

Myneni, R.B., Williams, D.L. 1994. On the relationships between FAPAR and NDVI. Remote Sens. Environ. 49: 200–211.

North. P.R.J. 1996. Three-dimensional forest light interaction model using a Monte Carlo method. IEEE Trans. Geosci. Electron. 34: 946–956.

North, P.R.J. 2002. Estimation of f_{APAR}, LAI, and vegetation fractional cover from ATSR-2 imagery. Remote Sens. Environ. 80: 114–121.

Olofsson, P., Eklundh, L. 2007. Estimation of abserbed PAR across Scandinavia from satellite measurments. Part II: Modeling and evaluating the fractional absorption. Remote Sens. Environ. 110: 240–251.

Orgaz, F., Villalobos, F.J., Testi, L., Fereres, E. 2007. A model of daily mean canopy conductance for calculating transpiration of olive canopies. Func. Plant Biol. 34: 178–188.

Oyarzun, R.A., Stöckle, C.O., Whiting, M.D. 2007. A simple approach to modeling radiation interception by fruit-tree orchards. Agr. Forest. Meteorol., 142: 12–24.

Pastor, M., García-Vila, M., Soriano, M.A., Vega, V., Fereres, E. 2007. Productivity of olive orchards in response to tree density. J. Hortic. Sci. Biotechnol. 82: 555–562.

Prieto-Blanco, A., North, P.R.J., Barnsley, M.J., Fox, N. 2009. Satellite-driven modelling of net primary productivity (NPP): theoretical analysis. Remote Sens. Environ. 113: 137–147.

Roujean, J.L., Breon, F.M. 1995. Estimating PAR absorbed by vegetation from bidirectional reflectance measurement. Remote Sens. Environ. 51: 375–384.

Stuckens, J., Somers, B., Delalieux, S., Verstraeten, W.W., Coppin, P. 2009. The impact of common assumptions on canopy radiativa transfer simulations: a case study in *Citrus* orchards. J. Quant. Spectrosc. Radiat. Transfer 110: 1–21.

Suárez, L., Zarco-Tejada, P.J., Berni, J.A.J., González-Dugo, V., Fereres, E. 2009. Modelling PRI for water stress detection using radiative transfer models. Remote Sens. Environ. 113: 730–744.

Suárez, L., Zarco-Tejada, P.J., González-Dugo, V., Berni, J.A.J.,Sagardoy, R., Morales, F., Fereres, E. 2010. Detecting water stress effects on fruit quality in orchards with time-serie PRI airborne imagery. Remote Sens. Environ. 114: 286–298.

Testi, L., Villalobos, F.J., Orgaz, F., Fereres, E. 2006. Water requirements of olive orchards. I. Simulation of daily evapotranspiration for scenario analysis. Irrig. Sci. 24: 69–76.

Villalobos, F.J., Orgaz, F., Mateos, L. 1995. Non-destructive measurement of leaf area in olive (*Olea europaea* L.) trees using a gap inversion method. Agr. Forest. Meteorol. 73: 29–42.

Villalobos, F.J., Testi, L., Hidalgo, J., Pastor, M. and Orgaz, F. 2006. Modelling potential growth and yield of olive (*Olea europaea* L.) canopies. Eur. J. Agron. 24: 296–303.

Vossen, P. 2007. Olive oil: history, production and characteristics of the world's classic oils. HortScience 42: 1093–1110

Wiegand, C.L., Richardson, A.J., Escobar, D.E., Gerbermann, A.H. 1991. Vegetation indices in crop assessments. Remote Sens. Environ. 35: 105–119.

Widlowski, J-L., Taberner, M., Pinty, B., Bruniquel-Pinel, V., Disney, M., Fernandez, R., Gastellu-Etchegorry, J-P., Gobron, N., Kuusk, A., Lavergne, T., Leblanc, S., Lewis, P.E., Martin, E., Mottus, M., North, P.R.J., Quin, W., Robustelli, M., Rochdi, N., Ruiloba, R., Soler, C., Thompson, R., Verhoef, W., Verstraete, M.M. and Xie, D. 2007. Third Radiation transfer Model Intercomparison (RAMI) exercise: documenting progress in canopy reflectance models. J. Geophys. Res. 112: D09111.

Widlowski, J-L., Pinty, B., Disney, M., Gastellu-Etchegorry, J-P., Lavergne, T., Lewis, P.E., North, P. R. J., Robustelli, M., Thompson, R. and Verstraete, M.M. 2008. The RAMI on-line model checker (ROMC): a web-based benchmarking facility for canopy reflectance models. Remote Sens. Environ. 112: 1144–1150.

Zhang, Q., Middleton, E.M., Margolis, H.A., Drolet, G.G., Barr, A.A., Black, T.A. 2009. Can a satellite-derived estimate of the fraction of PAR absorbed by chlorophyll ($FAPAR_{chl}$) improve predictions of light-use efficiency and ecosystem photosynthesis for a boreal aspen forest? Remote Sens. Environ. 113: 880–888.

Zarco-Tejada, P.J., Berjón, A., López-Lozano, R., Miller, J.R., Martín, P., Cachorro, V., González, M.R., Frutos, A. 2005. Assessing vineyard condition with hyperspectral indices: leaf & canopy reflectance simulation in a row-structured discontinuous canopy. Remote Sens. Environ. 99: 271–287.